2nd URSI AT-RASC, Gran Canaria, 28 May – 1 June 2018

Design and Test of a Toraldo Pupil Optical Module for the Medicina Radio Telescope

Luca Olmi(1), Pietro Bolli(1), Luca Carbonaro(1), Luca Cresci(1), Pasqualino Marongiu(2), Daniela Mugnai(3), Enzo Natale(1), Renzo Nesti(1), Dario Panella(1), Juri Roda(4) and Giampaolo Zacchiroli(4)
(1) Istituto Nazionale di Astrofisica (INAF), Osservatorio Astrofisico di Arcetri, Largo E. Fermi 5, I-50125 Firenze, Italy
olmi.luca@gmail.com
(2) Istituto Nazionale di Astrofisica (INAF), Osservatorio Astronomico di Cagliari, Via della Scienza 5, 09047 Selargius, Italy
(3) Consiglio Nazionale delle Ricerche (CNR), Istituto di Fisica Applicata Nello Carrara, Via Madonna del Piano 10, I-50019 Firenze, Italy
(4) Istituto Nazionale di Astrofisica (INAF), Istituto di Radioastronomia, Via P. Gobetti 101, I-40129 Bologna, Italy

Abstract

Toraldo Pupils (TPs) can improve the angular resolving power of an optical instrument beyond the classical diffraction limit (hence the term *super-resolution*) using a filter consisting of finite-width concentric coronae with different amplitude and phase transmittance. The first successful laboratory test of TPs in 2003 suggested that these devices could represent a viable approach to achieve super-resolution in Radio Astronomy. We have therefore started a project devoted to an exhaustive study of TPs and how they could be implemented on a radio telescope. In this work we present a summary of the design and laboratory tests of an optical module based on TPs that we plan to field-test on the Medicina 32-m radio telescope.

1 Introduction

The concept of super-resolution refers to various methods for improving the angular resolution of an optical imaging system beyond the classical diffraction limit. A feasible method to design antennas and telescopes with angular resolution better than the diffraction limit consists of using *variable transmittance pupils* which are also known as Toraldo variable transmittance pupils (TPs, hereafter) since they were introduced for the first time by G. Toraldo di Francia at a colloquium on optics and microwaves in 1952 [1].

We have therefore started a project devoted to a more complete analysis of TPs and how they could be implemented on a radio telescope. During the first part of this work we have conducted extensive electromagnetic (EM) numerical simulations of TPs, using the commercial software tool FEKO[1] [2]. We then used these EM simulations to conduct more comprehensive laboratory testing, aimed at confirming and expanding the first measurements carried out in the microwave range [3]. The experimental measurements, which are fully described elsewhere [4], showed that the super-resolution effect is achieved with two different types of TPs, and also showed a good agreement with the FEKO numerical simulations.

The next step in this project consists in the design and field-test of a prototype TP optical system to be mounted on a radio telescope. After analyzing various optical and mechanical constraints [5] we decided to design a TP optical module for the 18-26.5 GHz dual-horn receiver mounted at the Cassegrain focus of the 32-m Medicina antenna in Italy[2].

2 Design of the TP optical module

The design concept and performance, as well as the main mechanical and optical requirements of the TP module have already been discussed elsewhere [5]. The current design is based on a two-lens collimator placed after the Cassegrain focus (see Figures 1 and 2) and before the receiver dewar. The first lens of the collimator generates an image of the primary which is then brought to a subsequent focus by the second lens. The transmittance filter is placed at the image of the entrance pupil where it can modify the incident wavefront.

The baseline optical design of the collimator has been performed using standard Gaussian-beam propagation techniques and describing the transformation on the beam operated by the thick lenses using the ray transformation matrices, or ABCD matrices [6]. The input parameters to the optimization procedure are the beam-waist radius at the (modified) Cassegrain focus, which is placed at the focal position of the first lens, and the separation between the two lenses. The procedure then determines all other design parameters of the collimator, while keeping its maximum length within the allowed mechanical and optical constraints required by the mounting in the receiver cabin of the Medicina radio telescope. In Fig. 1 the curved paths trace the beam-waist radius, $w(z)$, as a function of the distance z from the Cassegrain focus. The green boxes represent the thickness and size of two plano-convex lenses, while the red

[1] http://www.altairhyperworks.com/product/FEKO

[2] http://www.med.ira.inaf.it/

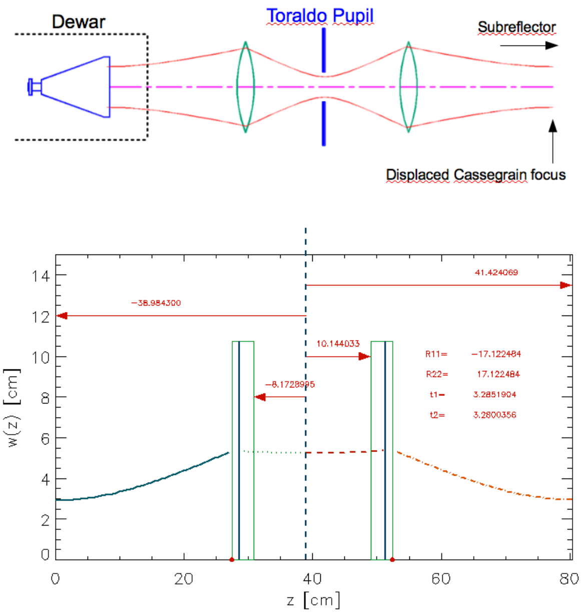

Figure 1. *Top panel.* Schematics of the collimator optics. The beam-waist at the modified Cassegrain focus is transformed by the two lenses and finally refocused on the feed-horn of the receiver. *Bottom panel.* Gaussian-beam propagation in the collimator on the upper half-plane (see text). The curved paths trace the beam-waist radius, $w(z)$, as a function of the distance z from the Cassegrain focus. The green boxes represent the thickness and size of two plano-convex lenses. The vertical lines inside the green boxes indicate the principal plane of the lens. The separation between various elements, radii of curvatures and thicknesses are also shown.

dots indicates the vertices of the lenses. The vertical lines inside the green boxes indicate the principal plane of the lens. Please note that the resulting optical system is not a Gaussian-Beam Telescope [6] since the separation between the two lenses is not equal to the sum of their focal lengths.

The initial optical and EM simulations of the collimator have been performed using a plano-convex lens shape. For the single curved surface we have analyzed both spherical and hyperboloidal profiles. For this first test TP module, we have not investigated the use of Fresnel lenses.

3 Fabrication and tests

To manufacture the (spherical) plano-convex lenses we used a computer numerical control milling machine (CNC). This fabrication technique enables to produce the lens from its digitized 3D description, by automatically excavating the object shape from a block of raw material (see Fig. 3). The lenses were fabricated from low-loss polyethylene, having a relative dielectric constant $\varepsilon_r = 2.28$ and a loss tangent of $\tan\delta \simeq 3.8\,10^{-4}$[6].

Our experimental measurements at this stage had three

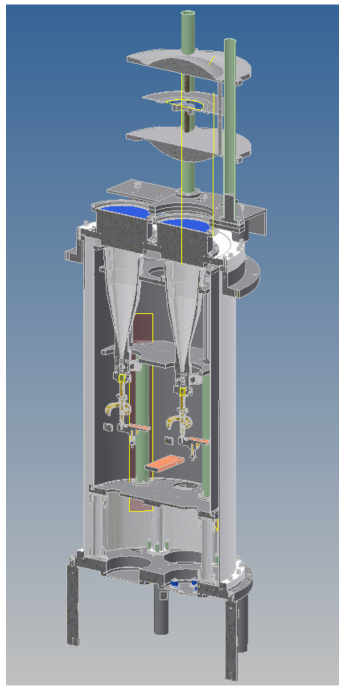

Figure 2. Design of the mechanical structure to mount the collimator on the dewar of the K-band dual-feed receiver.

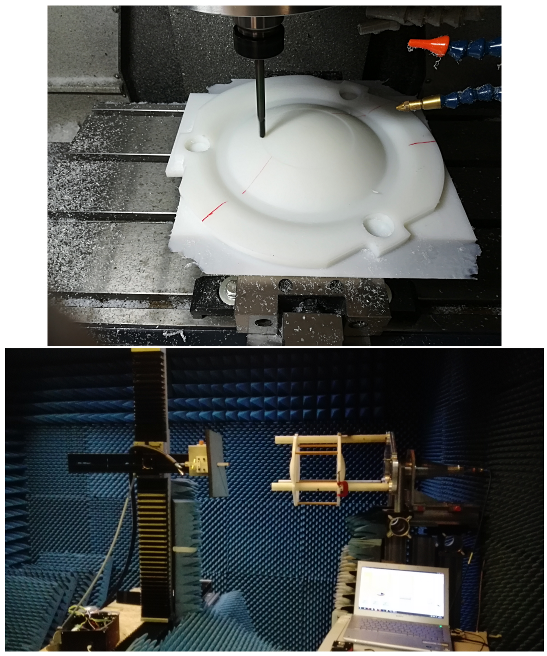

Figure 3. *Top panel.* Lens fabrication by CNC milling machine technique. *Bottom panel.* Experimental setup for our laboratory tests at $\nu = 20\,\mathrm{GHz}$. The launcher is visible to the right and to its left is placed the collimator with its support and aligning structure. Next, the NF probe is mounted on a two axis translation stage to scan the field perpendicularly to the direction of propagation, z. All components are mounted on vertical supports that can be moved along z on an optical bench set on the ground, which is covered with absorbing panels in this picture.

main goals: *(a)* verify the expected Gaussian-beam propagation properties of the corrugated feed-horn; *(b)* repeat the measurement adding a single lens to the optical system; *(c)* test the whole collimator setup with and without the TP. The laboratory tests were conducted in the anechoic chamber of the "Osservatorio Astrofisico di Arcetri" (INAF), where all microwave components were mounted on vertical supports that could move on an optical bench (see Fig. 3) along the direction of propagation (z-axis). All measurements were performed with a Vector Network Analyzer (VNA) recording both amplitude and phase. The launcher was a corrugated feed-horn, the same type mounted on the K-band receiver of the Medicina radio telescope. The near-field (NF) probe consisted of a section, 18cm in length, of an open-ended waveguide WR42 with smooth edges. Further details on the measurement setup can be found in Ref. [4].

The beam propagation properties of the K-band corrugated horn are shown in Fig. 4 and well reveals the differences between measurements and the ideal Gaussian-beam propagation. For each separate distance z from the feed-horn, we obtained separate fits to both the amplitude and phase measured at 41 separate points during either a x- or y-scan with the NF probe. The Gaussian fit to the measured amplitude allowed to obtain the full width at half maximum (FWHM) of the beam, while the quadratic fit to the phase allowed to obtain the radius of curvature, $R(z)$, of the beam using the relation giving the phase variation, $\phi(r)$, relative to a plane for a fixed value of z as a function of the offset, r, from the axis of propagation:

$$\phi(r) = \frac{kr^2}{2R} \quad (1)$$

where $k = 2\pi/\lambda$. The "+" symbols in Fig. 4 then represent the values of R obtained using this fitting technique, while the red curve represents $R(z)$ for an ideal Gaussian beam as given by:

$$R(z) = z + \frac{z_c^2}{z} \quad (2)$$

where $z_c = \pi w_o^2/\lambda$ is the confocal distance and w_o denotes the beam radius at $z = 0$, or beam waist radius. For our corrugated horn, the beam waist is located 22 mm (at $\nu = 20$ GHz) behind the aperture plane of the horn.

Figure 4 shows the difference between the ideal Gaussian-beam propagation and the experimental points. In order to test the effects of the waveguide probe used in the measurement process we built a FEKO model which would reproduce both the corrugated horn and the probe used to sample the NF. In this case, since the field detection is done only through the excitation of the waveguide, the EM simulation returns the values of the scattering parameters, or S-parameters, which measure the reflection and transmission coefficients through our VNA. The results of this simulation are shown by the green triangles in Fig. 4 which are consistent with the experimental points. For comparison we have also shown the results of the "standard" FEKO simulation (blue open squares) where the NF is sampled with an ideal

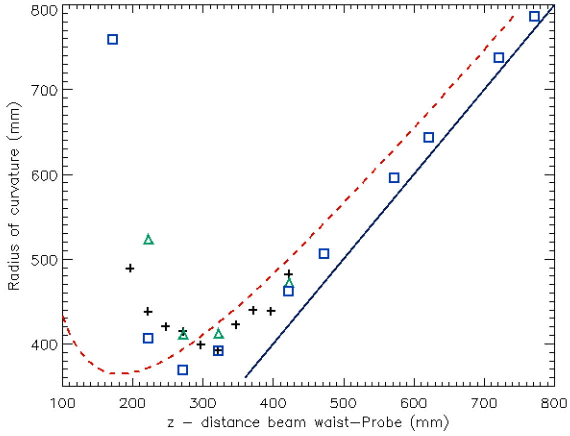

Figure 4. Radius of curvature, $R(z)$, of the Gaussian-beam radiated by the corrugated horn as a function of the distance, z, from the beam-waist inside the horn. The "+" symbols represent the laboratory measurements, the open triangles represent the FEKO results using the S-parameters, while the open squares represent the FEKO results using the modeled output fields. The red dashed curve represents the values of $R(z)$ for an ideal Gaussian-beam and the solid line corresponds to the asymptotic limit when $z \to \infty$.

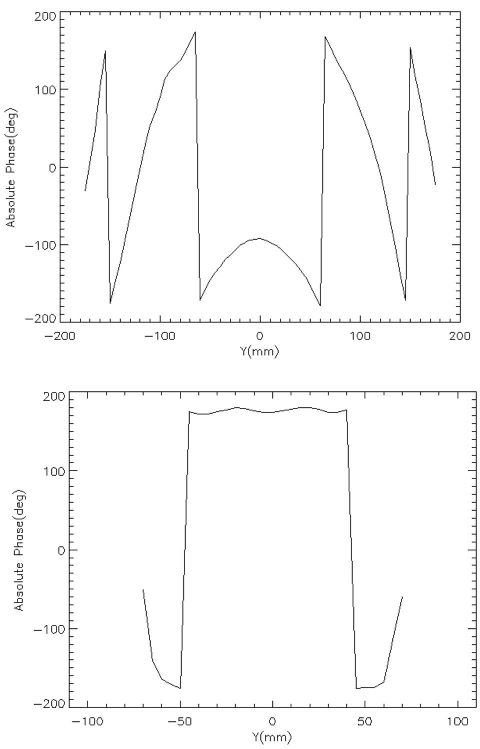

Figure 5. *Top panel.* y-scan of the phase of the field radiated by the corrugated horn, measured at a distance of 43 cm from the aperture. *Bottom panel.* y-scan of the phase inside the collimator, at the position where the TP would be placed. The distance from the feed-horn is the same as in the top-panel.

infinitely small probe. Although these points reproduce a minimum which is closer to that of the ideal $R = R(z)$ curve, we can still note some discrepancy, which is currently being analyzed.

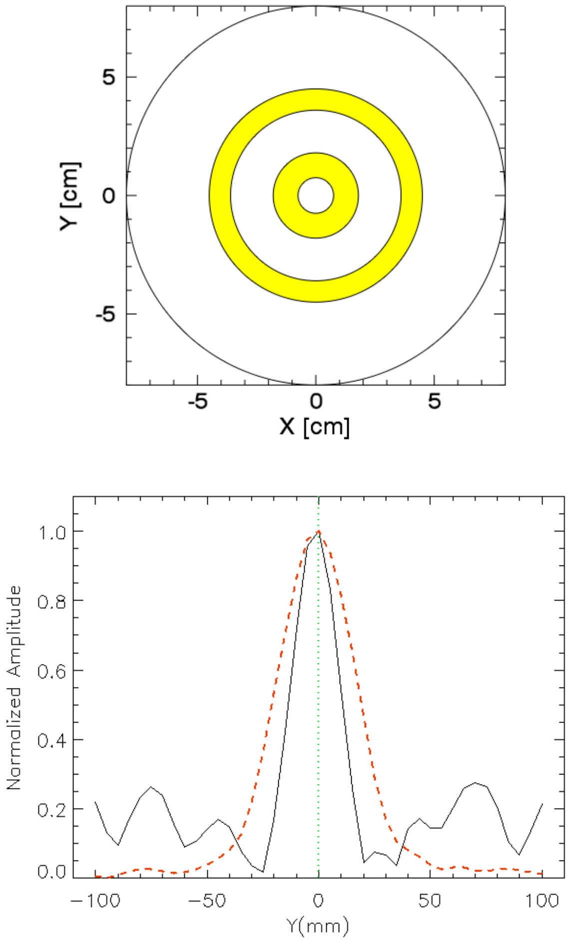

Figure 6. *Top panel.* Geometry of the five-coronae TP (or TP5) used in the laboratory measurements. The yellow areas correspond to the dielectric coronae. *Bottom panel.* Normalized measured amplitude at the output beam-waist of the collimator for the open pupil (red dashed curve) and the TP5 (black solid curve). Both amplitudes were measured at their peak positions.

Figure 5 shows how the collimator operates on the wavefront phase. The top panel shows the expected spherical shape of the wavefront phase at a distance of 43 cm from the aperture of the feed, which also corresponds to the distance of the TP position from the feed, when the collimator is in place. The middle panel shows the wavefront phase as measured at the TP position after the first lens of the collimator. One can clearly note that the phase is almost completely flat, as expected sine the first lens is supposed to convert a spherical wavefront into a plane one. Finally, the bottom panel shows the FWHM of the Gaussian beam after the second lens of the collimator, where the focusing action at the output of the collimator can be observed.

Finally, in Fig. 6 we show an example of the collimator output, with and without the TP5 mounted on the open pupil which is inserted between the two lenses. Both transverse $y-$scans were conducted at the position where the peak amplitude was previously found with a $z-$scan, corresponding to the output beam-waist. The point spread function (PSF) generated by the open pupil is clearly Gaussian, whereas the PSF obtained when the TP5 is present shows the typical expected high sidelobes of Toraldo pupils. The resulting super-resolution is visible, despite the TP5 shown here was not optimized for this configuration.

4 Acknowledgements

We gratefully acknowledge the partial support of the Ente Cassa di Risparmio di Firenze (Italy).

References

[1] G. Toraldo di Francia, *Il Nuovo Cimento (Suppl.)*, vol. 9, p. 426, 1952.

[2] L. Olmi, P. Bolli, L. Cresci, D. Mugnai, E. Natale, R. Nesti, D. Panella, and L. Stefani, "Super-resolution with Toraldo pupils: analysis with electromagnetic numerical simulations," in *Ground-based and Airborne Telescopes VI*, ser. Proc. SPIE, vol. 9906, 2016.

[3] D. Mugnai, A. Ranfagni, and R. Ruggeri, "Pupils with super-resolution," *Physics Letters A*, vol. 311, pp. 77–81, May 2003.

[4] L. Olmi, P. Bolli, L. Cresci, F. D'Agostino, M. Migliozzi, D. Mugnai, E. Natale, R. Nesti, D. Panella, and L. Stefani, "Laboratory measurements of super-resolving Toraldo pupils for radio astronomical applications," *Experimental Astronomy, submitted*, 2016.

[5] L. Olmi, P. Bolli, L. Carbonaro, L. Cresci, D. Mugnai, E. Natale, R. Nesti, D. Panella, J. Roda, and G. Zacchiroli, "Design of Super-Resolving Toraldo Pupils for Radio Astronomical Applications," in *General Assembly and Scientific Symposium of the International Union of Radio Science (URSI GASS), 2017 XXXIInd*, ser. IEEE Xplore, 2017.

[6] P. F. Goldsmith, *Quasioptical Systems*. New York: IEEE Press, 1998.